Reflectance and emission spectra of excitonic polaritons in GaN

K. Torii, T. Deguchi, T. Sota,* and K. Suzuki†
Department of Electrical, Electronics, and Computer Engineering, Waseda University, Shinjuku, Tokyo 169-8555, Japan

S. Chichibu‡
Faculty of Science and Technology, Science University of Tokyo, Yamazaki, Noda, Chiba 278-8510, Japan

S. Nakamura
Department of Research and Development, Nichia Chemical Industries Ltd., Oka, Kaminaka, Anan, Tokushima 744-8605, Japan
(Received 3 February 1999; revised manuscript received 20 May 1999)

High-resolution reflectance and emission spectra have been measured for high-quality free-standing GaN nearly free from residual strains and impurities. They have been analyzed based on a model exciton-polariton picture in which free *A*, *B*, and *C* excitons couple simultaneously to an electromagnetic wave, where the effective-mass anisotropy and the optical anisotropy are taken into account. Taking account of the free-exciton damping, we have calculated not only the dispersion relations but also the energy dependence of the imaginary part of the wave vectors for the excitonic polaritons. Furthermore, the lifetime of each polariton branch has been calculated combining the imaginary part of the polariton wave vectors and the group velocity obtained from the polariton dispersion relations. It is demonstrated that information on the polariton lifetime is indispensable for interpreting the emission spectra. A brief discussion will be given on obtained values for some physical parameters, including hole parameters. [S0163-1829(99)16131-9]

I. INTRODUCTION

The exciton polariton,[1,2] which is an elementary excitation consisting of free excitons and electromagnetic waves, is known to dominate optical properties of near-band edge in direct-gap semiconductors such as GaAs,[3–5] CdS,[5–7] and so on. Polariton effects in GaN have already been studied by two groups,[8,9] to the best of our knowledge. Gil, Clur, and Briot[8] discussed emission and reflection spectra at $T=2$ K from a GaN epitaxial layer grown on sapphire within coupled *A*, *B*, and *C* exciton-polariton pictures assuming isotropic exciton effective masses. Note that the GaN epitaxial layer grown on sapphire substrates suffers residual biaxial strain due to lattice mismatch between GaN and sapphire, though a part of strain is relaxed emitting high-density misfit dislocations. Stepniewski *et al.*[9] studied reflectance and emission spectra at $T=1.8$ K of high-quality, i.e., unstrained, homoepitaxial layers on GaN bulk crystals grown using a very high pressure of nitrogen. The observed reflectance spectra have been well reproduced by a theoretical calculation based on coupled *A*, *B*, and *C* exciton-polariton pictures assuming isotropic exciton effective masses, where the background dielectric function including contributions from the exciton excited states and from transitions between continuum states has been fully taken into account, as well as the existence of an exciton-free layer. However, the emission spectra in both reports are not so well resolved, probably because of the relatively high concentration of residual impurities. Thus discussions on the emission properties have been still insufficient in both reports.

Recently there has been a great demand for a GaN substrate with a large cross section, which can be used as lattice-matched substrates for optical and/or electronic devices. Such GaN substrates have been grown using lateral epitaxial overgrowth (LEO) techniques.[10–12] Sakai, Sunakawa, and Usui[13,14] found that the threading dislocations decrease drastically in the GaN substrate, and clarified the behavior of pure-edge, screw, and mixed dislocations. Reflectance and emission spectra at $T=5$ K of the LEO GaN substrate with various thickness were studied by Yamaguchi and co-workers.[15,16] They found a decrease of residual strain as the LEO GaN layer thickness increases, determined some important valence-band parameters, and showed the behavior of valence bands under uniaxial strain. However, they did not analyze their data based on the exciton-polariton picture, and their samples appear to include a considerable amount of residual impurities judging from the emission spectra. Therefore, it is of great interest to study polariton effects in the reflectance and emission spectra of a nearly intrinsic free-standing GaN of high quality.

In this paper high-resolution reflectance and emission spectra in the near-band-edge region are reported for a nearly intrinsic 70-μm-thick free-standing GaN grown using a LEO technique. The spectra are analyzed based on a model exciton-polariton picture in which *A*, *B*, and *C* excitons couple simultaneously to an electromagnetic wave, where effective-mass anisotropy and optical anisotropy are taken into account. The formulation allows one to determine both the real and imaginary parts of the complex wave vectors of the excitonic polaritons, taking into account the free-exciton dampings. Unknown physical parameters are determined to reproduce the reflectance spectra. Using obtained values for the physical parameters, we have calculated not only the dispersion curves but also the energy dependence of the imaginary part of the wave vectors of the excitonic polaritons. Using these, the lifetime of each exciton-polariton branch has been calculated to interpret the complex emission spectra. The information on the polariton lifetime indeed makes this interpretation easier. It is found that the complex emis-

sion spectra are well explained as the emission of excitonic polaritons accumulated at bottleneck portions of complex exciton-polariton branches. A part of hole parameters and the background dielectric constants obtained herein are also reported.

II. EXPERIMENTS AND RESULTS

A. Experimental

A sample was grown using the two-flow metal-organic chemical vapor deposition method.[17] Selective growth of GaN was carried out on a 2-μm-thick GaN layer grown on a (0001) C-face sapphire substrate under a low pressure of 100 Torr. The 0.1-μm-thick silicon dioxide (SiO_2) mask was patterned to form 4-μm-wide stripe windows with a periodicity of 11 μm in the GaN $\langle 1\bar{1}00 \rangle$ direction. Following the 10-μm-thick GaN growth on the SiO_2 mask patterns, the coalescence of the selectively grown GaN made it possible to achieve a flat GaN surface over the entire substrate. After obtaining a 10-μm LEO GaN, the GaN growth was continued up to a 100-μm thickness. After that the sapphire substrate and the LEO GaN including SiO_2 mask patterns were removed by polishing to obtain free-standing GaN with a thickness of approximately 70 μm. No film bending was observed. The resistivity of the sample was extremely high, indicating a small amount of residual impurities. Lattice constants measured by the Bond method were $a=3.1898 \pm 0.0002$ Å and $c=5.1855 \pm 0.0002$ Å, to demonstrate that the sample is nearly free from residual strain.[18] For a reference sample, we used a sample of 2-μm undoped GaN grown directly on a sapphire substrate via a low-temperature GaN buffer layer. The lattice constants of the sample were $a=3.1836 \pm 0.0002$ Å and $c=5.1898 \pm 0.0002$ Å. Here and hereafter, this sample is called a ''GaN on sapphire.''

Photoluminescence (PL) and reflectance spectra were measured at $T=10$ K. For reflectance measurements, a 150-W Xe lamp was used as a light source, and incident and the reflected angles θ were about 7° and 50°. Polarized experiments were also made using two Glan-Thomson prisms and a depolarizer for $\theta \approx 50°$. For PL measurements, photons with an energy larger than 3.2 eV from a 150-W Xe lamp, and second-harmonic photons of 3.52 eV from a Ti:sapphire laser with a repetition rate of 80 MHz and a pulse duration of 100 fs, were used as excitation sources for low and higher excitation conditions, respectively. PL signals emitted from the sample nearly along the surface normal were collected. The reflected and emitted light was dispersed by a $f=1.33$ m focal length monochrometer with 1800 grooves/mm holographic grating, whose entrance and exit slits were set to 20 μm. Signals were detected by a photomultiplier using phase-sensitive detection. The resolution was less than 0.01 nm in the whole wavelength region under investigation. The reflectance spectra were scaled with respect to the reflectivity of aluminum, and derived from the ratio of the reflection signals measured from the sample to that from the aluminum mirror, where the reflection coefficient of 0.93 for aluminum was taken into account as in Ref. 9. The reference reflectance spectrum was measured at room temperature but with the same experimental setup.

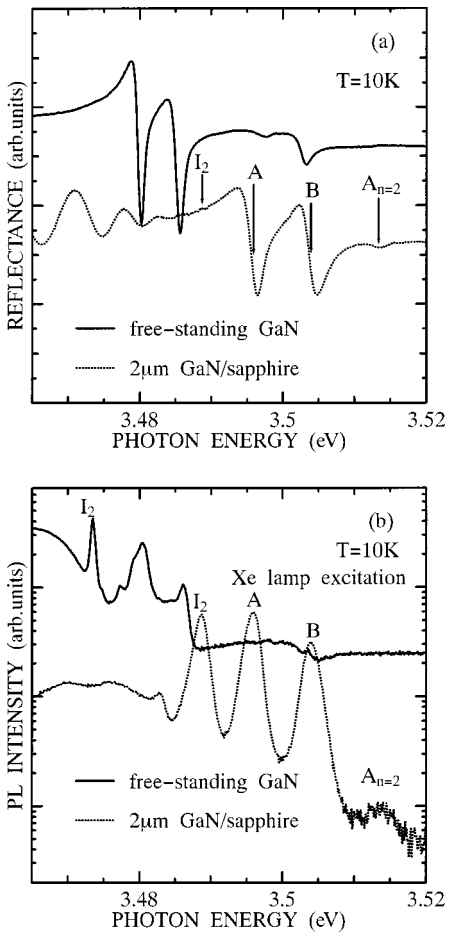

FIG. 1. Reflectance (a) and emission (b) spectra under Xe lamp excitation in free-standing GaN (solid curves) and 2-μm GaN on sapphire (dotted curves) at $T=10$ K. Energy positions labeled I_2, *A*, *B*, and $A_{n=2}$ in panel (a) denote the corresponding energy positions of emission peaks in the 2-μm GaN on sapphire shown in panel (b). In panel (b), I_2 indicates the emission from excitons bound to the neutral donors, the emission peaks *A* and *B* are due to the *A* and *B* free excitons judging from the almost Lorentzian-like line emission profiles, and the emission peak $A_{n=2}$ comes from the first excited states of the *A* exciton.

B. Experimental results

Figure 1 shows (a) reflectance ($\theta \approx 7°$) and (b) PL spectra of free-standing GaN, where those of GaN on sapphire are also shown for comparison. In Fig. 1(a), optical transitions corresponding to the ground states of the *A*, *B*, and *C* excitons are found around 3.480, 3.485, and 3.503 eV for the free-standing GaN, where the *C* exciton transition position was confirmed by polarization measurements, setting θ to 50°. The reflectance spectrum also reflects optical transitions corresponding to excited states of the excitons and those between valence bands to the conduction band. For GaN on sapphire, the *A* and *B* exciton ground-state transitions are found around 3.495 and 3.504 eV, respectively and a part of interference fringes are observed below 3.480 eV. It is clear from Fig. 1(a) that the structures corresponding to each optical transition become drastically sharper and shift toward the lower energy in the free-standing GaN than in the GaN on sapphire. The former reflects the decrease of homoge-

neous and inhomogeneous broadening, consequently, and the latter indicates the decrease of residual strain in the free-standing GaN.

It is found from Fig. 1(b) that the overall PL spectra shift toward the lower-energy region, to indicate the decrease of the residual strain as found in the reflectance spectra. For the free-standing GaN, the full width at half maximum of a neutral donor bound exciton peak, I_2, is 1.8 and 2.2 meV in the lower and higher excitation cases, respectively, though the PL spectrum under the higher excitation is not shown in Fig. 1(b). The ratio of the intensity of I_2 relative to that of PL peaks in the *A* and *B* exciton transition region is much smaller than that previously reported.[8,9,15] These indicate that the residual impurity concentration is sufficiently low, and this is consistent with the resistivity measurements. Judging from the facts that the emission profiles are almost the same as the Lorentzian line-shape functions, and that the linewidths are broad, the PL peaks of GaN on sapphire are regarded as emission peaks due to *A* and *B* free excitons. However, those of the free-standing GaN in the *A* and *B* exciton transition regions have complex structures, suggesting the formation of excitonic polaritons. Thus, to retain consistency, the reflectance spectra should also be analyzed based on an exciton-polariton model. The PL peaks near the transition from the first excited state of *A* and *B* excitons are not so well resolved. Emission from the *C* exciton ground state is dominantly allowed for the polarization $\vec{E}\|\vec{c}$, and is not probably observed in our experimental configuration.

III. CALCULATION OF REFLECTANCE SPECTRA

A. Formulation

To analyze and interpret the experimental data, a model calculation was carried out. Taking into account the simultaneous coupling of an electromagnetic wave with *A*, *B*, and *C* excitons, and the optical and the effective mass anisotropy in GaN which is the uniaxial crystal belonging to the space group C_{6v}^4, we start our calculation from the following equations:[5,6,9]

$$\left[\frac{\partial^2}{\partial t^2}+\omega_{0\nu}^2+\omega_{0\nu}\hbar\left(\frac{k_\perp^2}{M_{\nu\perp}}+\frac{k_\|^2}{M_{\nu\|}}\right)+\Gamma_\nu\frac{\partial}{\partial t}\right]\mathbf{P}_\nu=\omega_{0\nu}^2\overleftrightarrow{\alpha}_\nu\mathbf{E}, \tag{1}$$

$$\overleftrightarrow{\varepsilon}\mathbf{E}=\overleftrightarrow{\varepsilon}_0\mathbf{E}+4\pi\mathbf{P}, \tag{2a}$$

$$\mathbf{P}=\sum_\nu \mathbf{P}_\nu, \tag{2b}$$

where $\mathbf{E}$ is the electric field of light, and $\mathbf{P}(\mathbf{P}_\nu)$ the polarization due to the (νth) exciton. Equation (1) describes the equation of motion for the polarization contribution due to the νth exciton with the free-exciton resonance energy (the transverse exciton energy) $\hbar\omega_{0\nu}$, the damping constant Γ_ν, and the wave vector $k_\perp(k_\|)$, and the center of mass $M_{\nu\perp}(M_{\nu\|})$ perpendicular (parallel) to the c axis. Matrix representations are given for the polarizability tensor $\overleftrightarrow{\alpha}_\nu$, the residual dielectric function tensor $\overleftrightarrow{\varepsilon}_0$, excluding the contributions from the exciton ground states, and the dielectric function tensor $\overleftrightarrow{\varepsilon}$ as

$$\overleftrightarrow{\alpha}_\nu=\begin{pmatrix}\alpha_{\nu\perp} & & \\ & \alpha_{\nu\perp} & \\ & & \alpha_{\nu\|}\end{pmatrix},$$

$$\overleftrightarrow{\varepsilon}_0=\begin{pmatrix}\varepsilon_{0\perp}^*(\omega) & & \\ & \varepsilon_{0\perp}^*(\omega) & \\ & & \varepsilon_{0\|}^*(\omega)\end{pmatrix},$$

$$\overleftrightarrow{\varepsilon}=\begin{pmatrix}\varepsilon_\perp^*(\mathbf{k},\omega) & & \\ & \varepsilon_\perp^*(\mathbf{k},\omega) & \\ & & \varepsilon_\|^*(\mathbf{k},\omega)\end{pmatrix}, \tag{3}$$

where ω is the angular frequency of light. For the *A* exciton, $\alpha_{A\|}$ vanishes due to the symmetry of valence bands[19] within the lowest-order approximation.

From Eqs. (1) and (2), the following expressions for the dielectric function is derived:

$$\varepsilon_{\perp(\|)}(\mathbf{k},\omega)=\varepsilon_{0\perp(\|)}^*+\sum_\nu\frac{4\pi\omega_{0\nu}^2\alpha_{\nu\perp(\|)}}{-\omega^2+\omega_{0\nu}^2+\omega_{0\nu}\hbar k_0^2\left(\dfrac{\sin^2\theta}{M_{\nu\perp}}+\dfrac{(k/k_0)^2-\sin^2\theta}{M_{\nu\|}}\right)-i\omega\Gamma_\nu}, \tag{4}$$

where Snell's law is taken into account, and $k_0=\omega/c$ is the wave vector of light in vacuum (air). Equation (4) can be safely approximated as

$$\varepsilon_{\perp(\|)}(\mathbf{k},\omega)\approx\varepsilon_{0\perp(\|)}^*+\sum_\nu\frac{\omega_{0\nu}f_{\nu\perp(\|)}}{-\omega+\omega_{0\nu}+\dfrac{\hbar k_0^2}{2}\left(\dfrac{\sin^2\theta}{M_{\nu\perp}}+\dfrac{(k/k_0)^2-\sin^2\theta}{M_{\nu\|}}\right)-i\Gamma_\nu/2}, \tag{5}$$

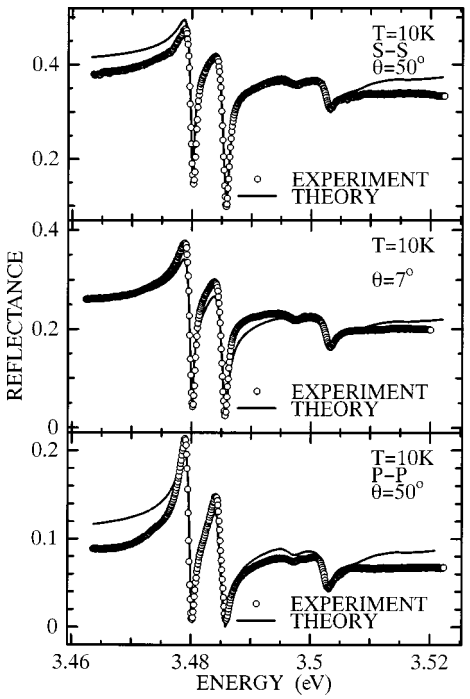

FIG. 2. Experimental (open dots) and theoretically calculated (solid curves) reflectance spectra in free-standing GaN at $T=10$ K. The middle panel represents the reflectance spectrum for near-normal incidence, i.e., an incident angle of 7°. Top and bottom panels represent the polarized reflectance spectra for the incident angle of 50°. $S-S$ $(P-P)$ denotes that both the incident and the reflected light have S (P) polarization.

with $f_{\nu\perp(\parallel)}=2\pi\alpha_{\nu\perp(\parallel)}$, because each oscillator plays a dominant role only in each resonance frequency region satisfying $|\omega-\omega_{0\nu}|\ll\omega_{0\nu}$. Equation (5) is also convenient for solving implicit dispersion relations shown below. The implicit dispersion relations are given by

$$\frac{\omega^2}{c^2}\varepsilon_\perp(\mathbf{k},\omega)-k^2=0 \tag{6a}$$

for the ordinary wave, and

$$\frac{\omega^2}{c^2}-\frac{k_\perp^2}{\varepsilon_\parallel(\mathbf{k},\omega)}-\frac{k_\parallel^2}{\varepsilon_\perp(\mathbf{k},\omega)}=0 \tag{6b}$$

for the extraordinary wave. The explicit dispersion relations can be obtained solving Eq. (6) numerically. After that, applying the electromagnetic boundary conditions and the additional boundary conditions (ABCs), in the present case Pekar[20] ABC's were used for the incident, refracted, and reflected waves; the effective refractive index of the medium, $\bar{n}$, is obtained after tedious but straightforward manipulations. Its explicit expressions is too complex to write herein. With respect to the calculational procedure, for example, see Ref. 4. The reflection coefficient R is given by

$$R=\left|\frac{1-\bar{n}}{1+\bar{n}}\right|^2. \tag{7}$$

TABLE I. Values of physical parameters obtained through the fitting procedure of the reflectance spectra. Values in parentheses are Ref. 9.

Parameters	Exciton *A*	Exciton *B*	Exciton *C*
$\hbar\omega_{0\nu}$(eV)	3.4791±0.0002	3.4844±0.0002	3.5027±0.0002
	(3.4767)	(3.4815)	(3.4986)
$f_{\nu\perp}$	0.0033±0.0003	0.0029±0.0003	0.00067±0.0003
	(0.0027)	(0.0031)	(0.0011)
$f_{\nu\parallel}$	0	0.0028±0.0004	0.00071±0.0001*
	(−)	(−)	(−)
Γ_ν(meV)	0.20±0.01	0.70±0.03	1.20±0.05
	(0.7)	(1.5)	(3.1)
$M_{\nu\perp}/m_0$	0.5*	0.6*	0.8*
	(1.0)	(1.0)	(1.0)
$M_{\nu\parallel}/m_0$	1.1±0.1	1.0±0.1	0.4*
	(1.0)	(1.0)	(1.0)
$E_{g\nu}$(eV)	3.5025	3.5080	-
	(3.497)	(−)	(−)
$E_{0\nu}$(meV)	23.44	23.6	-
	(20.3)	(20.3)	(20.3)
	[23.3]	[25.4]	[−]
$\Gamma_\nu(n\geqslant 2)$	1.8±0.1	1.5*	-
	(5.0)	(5.0)	(5.0)
		Background dielectric constants	
$\varepsilon_{0\perp}$		8.6	
$\varepsilon_{0\parallel}$		10.1	

TABLE II. Values for the valence-band parameters A_i $(i=1-4)$ in units of $\hbar^2/2m_0$ obtained in this paper. Note that the present results depend on the isotropic electron effective mass of $0.235m_0$. For comparison, previous theoretical results are also shown.

	A_1	A_2	A_3	A_4
Suzuki, Uenoyama, and Yanase [a]	−6.27	−0.96	5.70	−2.84
Kim *et al.*[b]	−6.4	−0.5	5.9	−2.55
Majewski, Stadle, and Vogl. [c]	−6.4	−0.8	5.93	−1.96
Yeo, Chong, and Li [d]	−7.24	−0.51	6.73	−3.36
Present	−6.21	−0.74	5.06	−3.04

[a]Reference 23.
[b]Reference 27.
[c]Reference 28.
[d]Reference 29.

Taking into account an exciton-free layer, the so-called ''dead layer,'' of thickness l, $\overline{n}$ is changed as[5]

$$\overline{n}=n_d\frac{(\overline{n_0}+n_d)\exp(-2ik_0n_dl)-n_d+\overline{n_0}}{(\overline{n_0}+n_d)\exp(-2ik_0n_dl)+n_d-\overline{n_0}}, \tag{8}$$

where n_d is the refractive index of the dead layer and $\overline{n_0}=\overline{n}(l=0)$. Strictly speaking, Eq. (8) is applicable only to the normal incidence. For oblique incidence, expressions of $\overline{n}$ for the s and p polarizations are different and should be distinguished. Concrete expressions for them are tedious and complex. Thus they are not shown here to save space.

The residual dielectric function should contain contributions from the static dielectric constant, oscillators describing resonance associated with the excited states of the A–C excitons, and those describing resonance between continuum states, as a first approximation.[9] Although the anisotropy should be taken into account for the three contributions, we use the isotropic expressions for the latter two contributions in calculations for simplicity. According to Haug and Koch,[21] the residual dielectric constants are expressed as

$$\begin{aligned}\varepsilon^*_{0\perp(\parallel)}(\omega)=\varepsilon_{0\perp(\parallel)}+\sum_\nu f_{\nu\perp(\parallel)}&\times\left[\sum_{n=2}^{\infty}\frac{1}{n^3}\frac{E_{0\nu}/\hbar}{-(\omega+i\delta_\nu)+(E_{g\nu}+E_{n\nu})/\hbar}\right.\\&+\frac{1}{2}\int_0^\infty dx\,\frac{x\exp(\pi/x)}{\sinh(\pi/x)}\\&\left.\times\frac{E_{0\nu}/\hbar}{-(\omega+i\delta_\nu)+(E_{g\nu}+E_{0\nu}x^2)/\hbar}\right],\end{aligned} \tag{9}$$

with $E_{n\nu}=-E_{0\nu}/n^2$ and $n=2,3,4,\ldots$, where $\varepsilon_{0\perp(\parallel)}$ is the background dielectric constant, $E_{0\nu}$ is the νth exciton binding energy, δ_ν is the excited-state linewidth of the νth exciton, $E_{g\nu}$ is the energy gap corresponding to the νth valence band, and x is a dummy variable with no dimension. Here the prefactor of the second and third terms in the right-hand side of Eq. (9) is replaced by $f_{\nu\perp(\parallel)}$ to keep consistency with Eq. (5). Those parameters are treated as fitting parameters. In numerical calculations, the upper limit for the integral of the third term on the right-hand side of Eq. (9) was replaced by an appropriate finite value avoiding divergence of the integral. The values of all parameters were obtained so as to achieve satisfactory agreement between the calculations and the experimental data.

B. Calculational results and discussions

The best-fit curves are shown for both cases of $\theta\approx 7°$ and 50° by solid curves in Fig. 2, where the experimental data are represented by open dots, squares, and diamonds for the spectrum at $\theta\approx 7°$, that with (s,s) polarization at $\theta\approx 50°$, and that with (p,p) polarization at $\theta\approx 50°$. Here the notation of (x,x) means that both the incident and reflected light have x polarization. Satisfactory agreement is achieved for all the spectra. Obtained values of physical parameters on the excitons and bands are summarized in Table I together with the previously reported values. Asterisks in Table I mean that the resultant reflection spectra are not sensitive to the physical parameter values with asterisks. The other parameter values are $l=6.0\pm 0.5$ nm and $x=50$.

It is found from Table I that each excitonic resonance energy in the free-standing GaN is slightly higher than that in the bulk GaN samples,[9] but is much lower than that in the GaN on sapphire, as mentioned above. This indicates the existence of a small but finite residual strain in the free-standing GaN. If not so, there is a possibility that the sample temperature in Ref. 9 was higher than 10 K. The obtained dead layer thickness is also reasonable, i.e., corresponding to the order of the exciton Bohr radius, but is larger by a small amount than that reported by Stepniewski *et al.*[9] The longitudinal-transverse splitting energies $\omega_{LT\nu}$ $(\nu=A,B,C)$ for the excitonic polaritons were estimated using the formula $\omega_{LT\nu}=f_{\nu\perp}\omega_{0\nu}/\varepsilon_{0\perp}$. The following values were obtained: $\hbar\omega_{LTA}=1.34$, $\hbar\omega_{LTB}=1.17$, and $\hbar\omega_{LTC}=0.273$ in units of meV. These values show a reasonable agreement with those in Ref. 9.

We obtained the effective masses for the center-of-mass motion of the A and B excitons. When the effective masses for electrons are known, we can determine the effective masses of A and B valence bands and some valence-band parameters within an assumption of zero strain. Furthermore, using those effective masses for electrons and holes, we can calculate the exciton binding energies. These calculations also check the consistency among the values for physical parameters obtained in this paper. We assume an isotropic

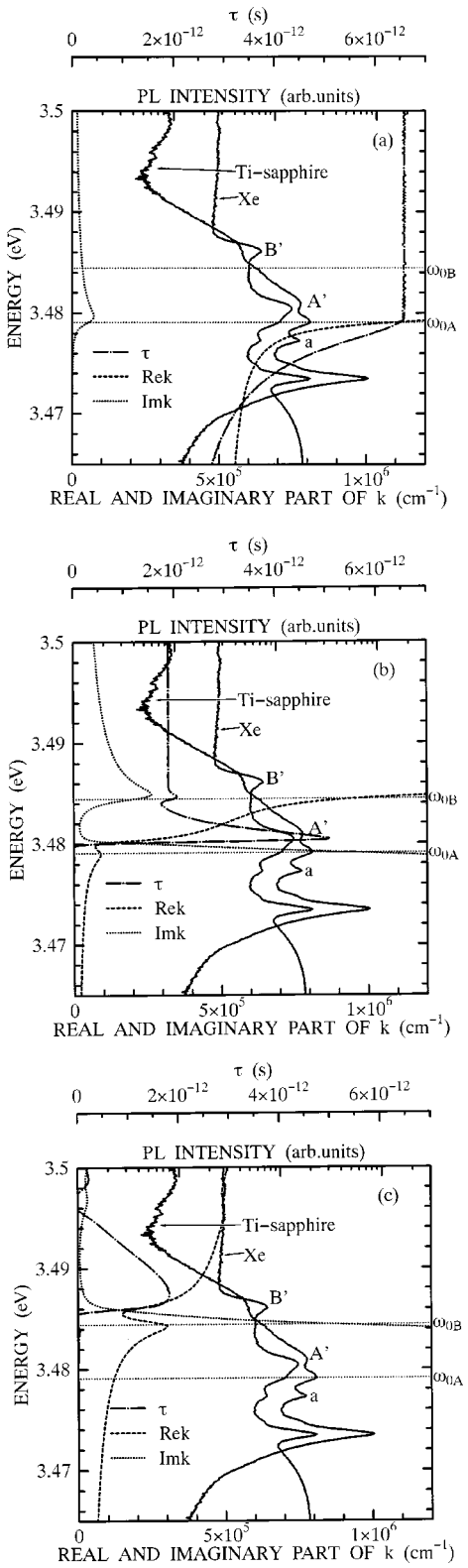

FIG. 3. Comparison of PL spectra at $T=10$ K with the exciton-polariton dispersion curves, $\hbar\omega$—k relation, for (a) LPB_A, (b) a branch combined UPB_A with LPB_B, and (c) a branch combined UPB_B with LPB_C, where LPB_α (UPB_α) means the lower (upper) polariton branch associated with the α exciton. The energy dependence of the imaginary part of the polariton wave vector Imk and of the polariton lifetime τ in each branch is also shown. Energy positions labeled ω_{0A} and ω_{0B} correspond to the resonance energies of the A and B free excitons.

effective mass for electrons of $0.235m_0$, which was determined by Knap *et al.*[22] using a cyclotron-resonance experiment in the GaN epilayer on sapphire. In calculating the exciton binding energy, the anisotropy of the background dielectric constants and the effective reduced masses are taken into account. The physical parameter values necessary for the calculations are taken from Table I. The calculated exciton binding energies are shown in square brackets in Table I. Although ambiguity remains in the value of $M_{\nu\perp}/m_0$, as mentioned above good agreement is achieved. Small discrepancies may be partly attributed to the ambiguity of the value of $M_{\nu\perp}/m_0$, and neglect of the anisotropy of electron effective masses. In any case, this calculation confirms the consistency among the values for the exciton binding energies for the A and B free excitons, the effective masses for the center-of-mass motion of those excitons, and the background dielectric constants, which are determined in this paper. Calculated values for the hole parameters, A_i ($i=1-4$), are listed in Table II, where those values obtained from first-principles calculations are also shown for comparison. The present parameter set is close to that calculated in Ref. 23, but definite conclusions cannot be drawn because of remained uncertainty mentioned above.

Here we would like to make the following comment. When the A exciton binding energy in the present free-standing GaN and that in the present GaN on sapphire are compared, the former is slightly larger than the latter. The A and B exciton binding energies are slightly larger than the previous reports by Shan *et al.*,[24] and Tchounkeu *et al.*,[25] but slightly smaller than that reported by Monemar *et al.*[26]

IV. INTERPRETATION OF EMISSION SPECTRA

The exciton-polariton dispersion relations are obtained by solving Eq. (6) numerically. Generally speaking, for the exciton-polariton problem, one searches the wave vector for a given energy. Taking the damping of excitons into account, the corresponding excitonic polariton may be attenuated under certain conditions. This is reflected in the fact that the solved wave vector becomes a complex number. Let k_r and k_i, respectively, be the real and imaginary parts of the wave vector k. The $\omega-k_r$ relation represents the exciton-polariton branches and the magnitude of each k_i, which, of course, varies depending on the energy, and indicates the degree of attenuation of the corresponding excitonic polariton. It is convenient to use the polariton lifetime in the time domain in interpreting the emission spectra. The polariton lifetime τ can be estimated from the relation $\tau=(k_i v_g)^{-1}$, where v_g is the group velocity of the corresponding polariton, and obtained as $v_g=\partial\omega/\partial k_r$.

Figure 3 compares the PL spectra with the $\omega-k_r$ relation, the $\omega-k_i$ relation, and the $\omega-\tau$ relation in (a) a lower polariton branch of the A exciton (LPB_A), (b) a branch combining an upper polariton branch of the A exciton (UPB_A) with a lower polariton branch of the B exciton (LPB_B), and (c) a branch combining an upper polariton branch of the B exciton (UPB_B) with a lower polariton branch of the C exciton (LPB_C). Here ω_{0A} and ω_{0B} denote the A and B free-exciton resonance energy, respectively. We focus our attention on the energy region between 3.465 and 3.490, because

the resolution of the emission spectra above 3.490 eV is not good.

We compare the PL spectra excited by the Xe lamp with the calculated $\omega-k_{r,i}$ and $\omega-\tau$ relations. It is found from Figs. 3(a) and 3(b) that there exist emission peaks corresponding to energies of $\hbar\omega_{0A}$ and $\hbar\omega_{0B}$. The value of τ at $\hbar\omega_{0A}$ is close to its maximum value in LPB_A, and the value of τ at $\hbar\omega_{0B}$ corresponds to the second maximum value of τ in LPB_B. Therefore, two emissions are assigned to the emissions of excitonic polaritons accumulated at the bottleneck portions in LPB_A and in LPB_B. Similarly, at the emission peak position labeled by A' (B'), the values of τ has its maximum value in UPB_A (UPB_B). Thus emissions A' and B' are assigned to those polaritons accumulated at the bottleneck portions in UPB_A and UPB_B. The energy difference between the emission peaks A (B) and A' (B') is about 1.3 (1.5) meV. This value shows reasonable agreement with the value of $\hbar\omega_{LTA}$ $(\hbar\omega_{LTB})$. This fact also supports the above assignments. The latter two polariton emission peaks show a blueshift when the excitation power is increased; see the PL spectra excited by the Ti:sapphire laser. This indicates that many more excitonic polaritons accumulate at the bottleneck portions under the higher power excitation condition. However, the two polariton emission peaks at $\hbar\omega_{0A}$ and $\hbar\omega_{0B}$ show no remarkable blueshift. This is probably because the curvatures of the corresponding $\omega-k_r$ relations are smaller for them than for A' and B' polaritons. It is interesting that polaritons leading to those four emission peaks suffer from rather stronger attenuation when they propagate spatially, see the $\omega-k_i$ relations.

The remaining emission peak to be assigned is that labeled a. As far as the present model exciton-polariton picture is used, there is no reason to assign its origin as polariton emission. Its energy separation from the I_2 peak is 3.9 meV. A similar emission peak was found by Pakula *et al.*,[30] where the peak position was separated from the I_2 peak position by 3.6 meV. They assigned this to impurity-related emission.[30] Following their example, we tentatively assumed the origin of the emission to be an impurity-related one.

V. CONCLUSION

We have carried out measurements of reflectance and emission spectra from a pure free-standing GaN, to obtain well-resolved spectra. We have determined the values of physical parameters associated with the excitons, the valence bands, and so on. The $\omega-k_{r,i}$ and $\omega-\tau$ relations calculated using these measurements have been used to interpret the complex emission structures corresponding to the A and B exciton regions, to be able to specify the origin of all the peaks. It has been demonstrated that information on polariton lifetime is indispensable to interpret the complex emission spectra.

ACKNOWLEDGMENTS

We are grateful to Dr. Uenoyama for his critical reading of the manuscript and for stimulating discussions. One of us (S.C.) is also grateful to Professor H. Nakanishi (SUT), and Professor S. P. DenBaars (UCSB) for their continuous encouragement. This work was supported in part by the Ministry of Education, Science, Sports, and Culture of Japan (High-Tech Research Center Project) and by the Japan Society for the Promotion of Science (''Research for the Future'' Program No. JSPS-RFTF96P00103).

*Also at the Material Research Laboratory for Bioscience and Photonics, Graduate School of Science and Engineering, Waseda University, Shinjuku, Tokyo 169-8555, Japan. Electronic address: sota@elec.waseda.ac.jp

†Also at the Kagami Memorial Laboratory for Material Science and Technology, Waseda University, Shinjuku, Tokyo 169-8555, Japan.

‡Present address: Department of Applied Physics, University of Tsukuba, 1-1-1 Tengendai, Tsukuba, Ibaraki 305-8573, Japan. Electronic address: chichibu@ims.tsukuba.ac.jp

[1] J. J. Hopfield, Phys. Rev. **112**, 1555 (1958).

[2] Y. Toyozawa, Prog. Theor. Phys. Suppl. **12**, 111 (1959).

[3] T. Steiner, M. L. W. Thewalt, E. S. Coteles, and J. P. Salerno, Phys. Rev. B **34**, 1006 (1986).

[4] D. Sell, S. E. Stokowski, R. Dingle, and J. V. DiLorenzo, Phys. Rev. B **7**, 3468 (1973).

[5] For a review, for example, see *Excitons*, edited by V. M. Agranovich and A. A. Maradudin, Modern Problems in Condensed Matter Physics Vol. 2 (North-Holland, Amsterdam, 1982).

[6] J. J. Hopfield and D. G. Thomas, Phys. Rev. **132**, 563 (1963).

[7] J. Lagois, Phys. Rev. B **16**, 1699 (1977).

[8] B. Gil, S. Clur, and O. Briot, Solid State Commun. **104**, 267 (1997).

[9] P. Stepniewski, K. P. Korona, A. Wysmolek, J. M. Baranowski, K. Pakula, M. Potemski, G. Martinez, I. Grzegory, and S. Porowski, Phys. Rev. B **56**, 15 151 (1997).

[10] A. Usui, H. Sunakawa, A. Sakai, and A. A. Yamaguchi, Jpn. J. Appl. Phys. **36**, L899 (1997).

[11] O. H. Nam, M. D. Bremser, T. Zheleva, and R. F. Davis (unpublished).

[12] S. Nakamura, M. Senoh, S. Nagahama, N. Iwasa, T. Yamada, T. Matsushita, H. Kiyoku, Y. Sugimoto, T. Kozaki, H. Umemoto, M. Sano, and K. Chocho, Jpn. J. Appl. Phys. **37**, L309 (1998).

[13] A. Sakai, H. Sunakawa, and A. Usui, Appl. Phys. Lett. **71**, 2259 (1997).

[14] A. Sakai, H. Sunakawa, and A. Usui, Appl. Phys. Lett. **73**, 481 (1998).

[15] A. A. Yamaguchi, Y. Mochizuki, H. Sunagawa, and A. Usui, J. Appl. Phys. **83**, 4542 (1998).

[16] A. A. Yamaguchi, Y. Mochizuki, C. Sasaoka, A. Kimura, M. Nido, and A. Usui, in *Nitride Semiconductors*, edited by F. A. Ponce *et al.*, MRS Symposia Proceedings No. 482 (Materials Research Society, Pittsburgh, 1998), p. 893.

[17] For a review, see S. Nakamura and G. Fasol, *The Blue Laser Diode* (Springer-Verlag, Heidelberg, 1997).

[18] M. Leszczynski, T. Suzuki, P. Peerlin, H. Teisseyre, I. Grzegory, X. Bockowski, J. Jun, S. Porowski, and J. Major, J. Phys. D **28**, A149 (1995).

[19] G. L. Bir and G. E. Pikus, in *Symmetry and Strain-Induced Effects in Semiconductors* (Wiley, New York, 1974).

[20] S. I. Pekar, Zh. Éksp. Teor. Fiz. **33**, 1022 (1957) [Sov. Phys. JETP **6**, 785 (1958)].

[21] H. Haug and S. W. Koch, *Quantum Theory of Optical and Elec-*

tronic Properties of Semiconductors (World Scientific, Singapore, 1990), p. 194.
[22] W. Knap, S. Conotreras, H. Alause, C. Kierbiszwski, J. Camassel, M. Dyakonov, J. Yang, Q. Che, M. Asif-Khan, M. L. Sadoeski, S. Huant, F. H. Yang, M. Goiran, J. Leotin, and M. S. Shur, Appl. Phys. Lett. **70**, 2123 (1997).
[23] M. Suzuki, T. Uenoyama, and A. Yanase, Phys. Rev. B **52**, 8132 (1995).
[24] M. Shan, B. D. Little, J. J. Song, B. Goldenberg, W. G. Perry, M. D. Bremser, and R. F. Davis, Phys. Rev. B **54**, 16 369 (1996).
[25] M. Tchounkeu, O. Briot, B. Gil, J. P. Alexis, and R. L. Aulombard, J. Appl. Phys. **80**, 5352 (1996).
[26] B. Monemar, J. E. Bergman, L. A. Buyanov, W. Li, H. Amano, and I. Akasaki, *MRS Internet J. Nitride Semiconductor Res.* **1**, 2 (1996).
[27] K. Kim, W. R. L. Lambercht, B. Segall, and M. van Schilfgaarde, Phys. Rev. B **56**, 7363 (1997).
[28] J. A. Majewski, M. Stadle, and O. Vogl, in *III-V Nitrides*, edited by F. A. Ponce, T. D. Moustakas, I. Akasaki, and B. Monemar, MRS Symposia Proceedings No. 449 (Materials Reserch Society, Pittsburgh, 1997), p. 887.
[29] Y. C. Yeo, T. C. Chong, and M. F. Li, in *III-V Nitrides* (Ref. 28), p. 923.
[30] K. Pakula, A. Wysmolek, K. P. Korona, J. M. Baranowski, I. Grzegory, M. Bockowski, J. Jun, S. Krukowski, M. Wroblewski, and S. Porowski, Solid State Commun. **97**, 919 (1996).